



## Short-range correlations and the charge density

Ronen Weiss<sup>a,\*</sup>, Axel Schmidt<sup>b</sup>, Gerald A. Miller<sup>c</sup>, Nir Barnea<sup>a</sup>

<sup>a</sup> The Racah Institute of Physics, The Hebrew University, Jerusalem, Israel

<sup>b</sup> Massachusetts Institute of Technology, Laboratory for Nuclear Science, Cambridge, MA 02139, USA

<sup>c</sup> University of Washington, Department of Physics, Seattle, WA 98195, USA



### ARTICLE INFO

#### Article history:

Received 2 August 2018

Received in revised form 6 December 2018

Accepted 28 January 2019

Available online 31 January 2019

Editor: W. Haxton

#### Keywords:

Short range correlations

Contact formalism

Charge density

### ABSTRACT

Sophisticated high-energy and large momentum-transfer scattering experiments combined with ab-initio calculations can reveal the short-distance behavior of nucleon pairs in nuclei. On an opposite energy and resolution scale, elastic electron scattering experiments are used to extract the charge density and charge radius of different nuclei. We show that even though the charge density has no obvious connection with nuclear short-range correlations, it can be used to extract properties of such correlations. This is accomplished by using the nuclear contact formalism to derive a relation between the charge density and the proton–proton nuclear contacts that describe the probability of two protons being at close proximity. With this relation, the values of the proton–proton contacts are extracted for various nuclei using only the nuclear charge density and a solution of the two-nucleon Schroedinger equation as inputs. For symmetric nuclei, the proton–neutron contacts can also be extracted from the charge density. Good agreement is obtained with previous extractions of the nuclear contacts. These results imply that one can predict (with reasonably good accuracy) the results of high-energy and large momentum-transfer electron-scattering experiments and ab-initio calculations of high momentum tails using only experimental data of elastic scattering experiments.

© 2019 The Authors. Published by Elsevier B.V. This is an open access article under the CC BY license (<http://creativecommons.org/licenses/by/4.0/>). Funded by SCOAP<sup>3</sup>.

Many efforts have been devoted in the last couple of decades to the study of nuclear short-range correlations (SRCs) and the short-range properties of the nuclear force. Sophisticated high-energy and large momentum-transfer electron and proton scattering experiments [1–11], together with ab-initio calculations [12–20], were performed. This led to a good understanding of the main properties of nuclear SRCs. For example, the dominance of neutron–proton pairs due to the significant nuclear tensor force was identified. Calculations of momentum distributions of different nuclei revealed high momentum tails similar in shape to the deuteron high momentum tail, showing the universal aspects of SRCs. Nevertheless, ab-initio numerical calculations are limited to light and medium-size nuclei, and only recently SRCs calculations for <sup>40</sup>Ca became accessible. In addition, experimental data are only available for selected nuclei. See also recent reviews [21–23].

Significant progress in the study of SRCs was made in the field of atomic physics when the contact theory was presented [24]. A single parameter, called the contact, describing the probability

to find two atoms close to each other, was shown to be related to many other properties of the atomic system [25]. Some of these relations are intuitive, such as a relation between the contact and the high momentum tail of the momentum distribution. Others, however, are less intuitive, such as relationships between the contact parameter and thermodynamic properties of the system, for instance, the energy of the system, its pressure, and its entropy. See also Ref. [26] for improvements in a few of these relations.

The contact formalism was recently generalized to nuclear systems [27–30]. The nuclear contacts were defined, and were shown to be related to many different nuclear quantities, such as the two-nucleon density [30], high momentum tails [28,30,31], the Coulomb sum-rule [32], the Lvinger constant [27,33], and electron scattering experiments [34]. However, the corresponding connection between the nuclear contacts and the low-energy or thermodynamic nuclear properties was not discovered.

Here, we use the nuclear contact formalism to show that nuclear SRCs and the nuclear charge-density, closely related to the one-body proton density, do indeed have direct connection. This is surprising because the charge density of a given nucleus is measured in elastic scattering experiments that are much simpler than the high-energy experiments devoted to the study of SRCs. The charge density and charge radius of nuclei can be explained using

\* Corresponding author.

E-mail addresses: [ronen.weiss1@mail.huji.ac.il](mailto:ronen.weiss1@mail.huji.ac.il) (R. Weiss), [nir@phys.huji.ac.il](mailto:nir@phys.huji.ac.il) (N. Barnea).

mean field theories, i.e. without an explicit need for nuclear SRCs. Experimental results of the charge density are available for many nuclei, see e.g. Ref. [35]. Therefore, it might seem that the charge density and SRCs are two unrelated aspects of nuclear systems. To connect these two entities we use both the charge density and the contact formalism to build a simple model for the proton–proton pair density  $\rho_{pp}(\mathbf{r})$ , i.e. for the probability of finding two protons separated by a distance  $\mathbf{r}$ . Assuming only the continuity of the proton–proton pair density, we obtain a direct relation between the nuclear contacts and the charge density. Since the charge density of many nuclei is known experimentally, this new relation can be used to understand the properties of nuclear SRCs of nuclei that are not reachable by ab-initio calculations or not yet studied experimentally in SRC experiments.

The two main building blocks of the nuclear contact formalism are the contacts and the universal functions  $\varphi_{ij}^\alpha(r)$ , with the index  $ij$  representing the three possible pairs of nucleons: proton–proton ( $pp$ ), proton–neutron ( $pn$ ) and neutron–neutron ( $nn$ ) and  $\alpha$  the quantum numbers of the pair. The universal functions describe the motion of a pair of nucleons being close to each other inside the nucleus, interacting mostly with each other, and not with the rest of the nucleons in the system. They can be simply calculated by solving the two-nucleon Schroedinger equation for zero-energy with a given nucleon–nucleon potential. The two most significant channels are [30]: the spin-zero  $s$ -wave channel, occupied by all three kinds of pairs ( $pp$ ,  $pn$  and  $nn$ ) and denoted by  $\alpha = 0$ , and the spin-one deuteron channel ( $s$ -wave and  $d$ -wave coupled), occupied only by  $pn$  pairs and denoted by  $\alpha = 1$ . Here, the nucleon–nucleon AV18 potential [36] is used for the calculation of the universal functions.  $\varphi_{ij}^\alpha(r)$  are normalized such that  $\int_{k_F}^\infty |\tilde{\varphi}_{ij}^\alpha(\mathbf{k})|^2 d\mathbf{k}/(2\pi)^3 = 1$ , where  $\tilde{\varphi}_{ij}^\alpha(\mathbf{k})$  is the Fourier transform of  $\varphi_{ij}^\alpha(r)$ , and  $k_F = 1.3 \text{ fm}^{-1}$ .

The nuclear contacts are generally matrices denoted by  $C_{ij}^{\alpha\beta}$ , but we will focus here only on the diagonal elements  $C_{ij}^\alpha$ , which are proportional to the probability of finding an  $ij$  pair in the channel  $\alpha$  close to each other in the nucleus. The values of the contacts are nucleus-dependent, while the two-body functions  $\varphi_{ij}^\alpha(r)$  are identical for all nuclei. As mentioned above, several relations connecting these nuclear contacts and different nuclear quantities and reactions have been derived. Thus, given the values of the contacts, different experimental and numerical results can be described. Recently, the values of the contacts for several  $A \leq 40$  nuclei have been extracted [30], from available Variational Monte Carlo (VMC) calculations [37,38]. Obtaining the values of the contacts is still a challenge for heavier nuclei. We note that the description of SRCs using the contacts and the universal functions is based on the asymptotic factorization of the total wave function [28]. The wave function of the VMC method is built as a product of Jastrow correlation functions [37], resembling the assumed factorization. Therefore, the asymptotic factorization should be further investigated using other ab-initio methods, but this goes beyond the scope of this work.

We now connect nuclear SRCs with the charge density using a simple description of the two-body  $pp$  pair-density. The  $pp$  pair-density  $\rho_{pp}(\mathbf{r})$  describes the probability to find a  $pp$  pair at a relative distance  $r$  in a given nucleus, and is normalized to the total number of  $pp$  pairs, i.e.  $\int d\mathbf{r} \rho_{pp}(\mathbf{r}) = Z(Z-1)/2$ . For small distances, this density is clearly related to short-range correlations, and can be expressed using the nuclear contacts [30]

$$\rho_{pp}(\mathbf{r}) = C_{pp}^0 |\varphi_{pp}^0(\mathbf{r})|^2. \quad (1)$$

Previous work [30] found that this relation holds for  $r < r_0 \approx 0.9 \text{ fm}$  for nuclei with  $A \leq 40$ .

For large separation distances, we expect that no correlations will be relevant and thus the two-body  $pp$  pair-density can be written using the one-body point-proton density  $\rho_p(\mathbf{r})$  [39]:

$$\rho_{pp}(\mathbf{r}) \propto \rho_{pp}^{UC}(\mathbf{r}) \equiv \int d\mathbf{R} \rho_p(\mathbf{R} + \mathbf{r}/2) \rho_p(\mathbf{R} - \mathbf{r}/2), \quad (2)$$

integrating over all possible locations of the center-of-mass  $\mathbf{R}$  of the  $pp$  pair. This asymptotic behavior does not account for the fermionic nature of the  $pp$  pair. To understand its effect, we examine the Fermi-gas model for infinite nuclear matter having a constant proton density  $\rho_p$ . In this model, the probability to find two protons at positions  $\mathbf{r}_1$  and  $\mathbf{r}_2$  is given by

$$\rho_{pp}(\mathbf{r}_1, \mathbf{r}_2) = \frac{1}{2} \rho_p^2 \left[ 1 - \frac{1}{2} \left( \frac{3j_1(k_F^p r)}{k_F^p r} \right)^2 \right], \quad (3)$$

where  $j_1$  is a spherical Bessel function,  $r = |\mathbf{r}_1 - \mathbf{r}_2|$  and  $k_F^p$  is the proton Fermi momentum. Based on this expression, and integrating over the center of mass of the pair  $\mathbf{R} = \mathbf{r}_1 + \mathbf{r}_2$ , we expect that the  $pp$  density of finite nuclei at large distances will obey

$$\rho_{pp}(r) \xrightarrow{r \rightarrow \infty} \rho_{pp}^F(r) \equiv \mathcal{N} \rho_{pp}^{UC}(r) \left[ 1 - \frac{1}{2} \left( \frac{3j_1(k_F^p r)}{k_F^p r} \right)^2 \right]. \quad (4)$$

Here,  $\mathcal{N}$  is a normalization factor, fixing the normalization of  $\rho_{pp}^F(r)$  to the number of  $pp$  pairs. This provides an asymptotic expression for the  $pp$  density that can be calculated directly from the one-body point-proton density. The charge density, measured in elastic scattering experiments, is slightly different than the point-proton density, due to the structure of protons and neutrons and their internal charge distribution. Nevertheless, for medium-size and heavy nuclei this difference becomes small, and the experimental charge distribution can be used in Eq. (2) to a good approximation. In addition, since Eq. (4) is based on the nuclear matter expression, we might not expect it to hold for the light nuclei. Shell model calculations for  $^{16}\text{O}$  using harmonic oscillator orbitals (with  $\sqrt{\hbar/m\omega} = 1.79 \text{ fm}$ , following Ref. [40]) agree with the plane-wave nuclear matter correction (used in Eqs. (3) and (4)). For  $k_F^p = 0.9 \text{ fm}^{-1}$  less than 2% difference is seen for  $r < 4 \text{ fm}$ , and for a more realistic value of  $k_F^p = 1.05 \text{ fm}^{-1}$  an agreement with 10% accuracy is obtained for the same range.

If SRCs were not significant in nuclear systems, then  $\rho_{pp}^F(r)$  might have been a good approximation for the exact  $\rho_{pp}(r)$  for all  $r$ . Thus, we can expect that the asymptotic expression of Eq. (4) will hold for  $r \gtrsim r_0$ , because SRCs are significant for  $r \lesssim r_0$ .

We now have expressions for both small-distance and large-distance asymptotics of  $\rho_{pp}(r)$  that can be compared to results of available VMC numerical calculations [37,38], calculated using the AV18 [36] and UX [41] potentials. The results for  $^{40}\text{Ca}$  are presented in Fig. 1. First observe that the uncorrelated  $\rho_{pp}^{UC}$ , calculated using either the VMC point-proton density or experimental charge distribution [35], coincides with the VMC  $pp$  density for large distances ( $r \gtrsim 3 \text{ fm}$ ). Then note that the uncorrelated  $pp$  density including the Fermi statistic  $\rho_{pp}^F$  describes (as expected) the full  $\rho_{pp}$  density for  $r \gtrsim r_0$  reasonably well. For smaller separations the contact relation, Eq. (1), using the AV18 potential, is seen to agree with the VMC calculations for  $r \lesssim r_0$ . Most importantly, one can see that around  $r_0 \approx 0.9 \text{ fm}$  both the contact and the  $\rho_{pp}^F$  expressions seem to describe the value of the full  $\rho_{pp}$  reasonably well.

The Fermi momentum is calculated via its relation to the proton density. For infinite nuclear matter  $k_F^p = (3\pi^2 \rho_p)^{1/3}$ . For finite nuclei,  $\rho_p$  depends on the location. In the local density approximation, the Fermi momentum at the pair's center of mass  $\mathbf{R}$  is given by

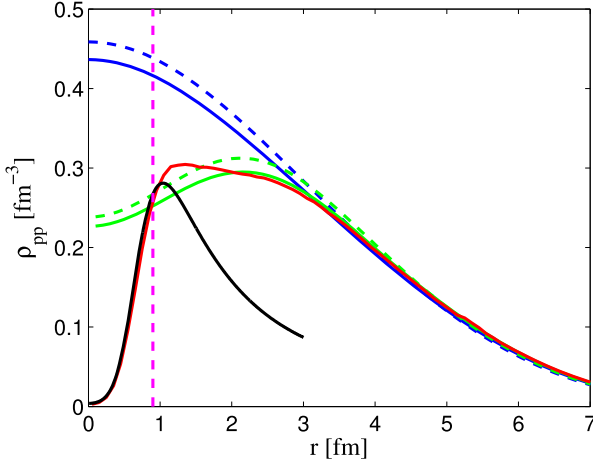


**Fig. 1.** The  $pp$  density for  $^{40}\text{Ca}$ . The red line shows the full  $pp$  density  $\rho_{pp}$  of the VMC calculations [38]. The blue lines show the calculated  $\rho_{pp}^{UC}$ , based on Eq. (2), using the one-body point-proton density of the VMC calculations (solid) or the experimental charge density (dashed), using the three-parameter Fermi model [35]. The green lines show the corresponding uncorrelated  $pp$  density with the Fermi-statistic correction, using Eq. (4). The black line shows the contact expression for the  $pp$  density, using the AV18 potential and the contact value extracted in Ref. [30] by fitting to the VMC data in coordinate space. The blue, green and red lines are all normalized to the number of  $pp$  pairs. The vertical magenta line shows the location of  $r = 0.9$  fm.

$$k_F^p(\mathbf{R}) = (3\pi^2 \rho_p(\mathbf{R}))^{1/3}. \quad (5)$$

We can use this expression of the proton Fermi momentum  $k_F^p(\mathbf{R})$  for evaluating Eq. (3), or instead we can use the weighted average value

$$k_F^p = \frac{\int d\mathbf{r} k_F^p(\mathbf{r}) \rho_p(\mathbf{r})}{\int d\mathbf{r} \rho_p(\mathbf{r})}. \quad (6)$$

In the calculations presented in Fig. 1, we have used this last relation resulting in a numerical value of  $k_F^p \approx 1.05 \text{ fm}^{-1}$  for  $^{40}\text{Ca}$ . Another possible choice for  $k_F^p$  is to use the value of  $\rho_p(r)$  at the center of the nucleus, i.e.  $r = 0$ ,

$$k_F^p = (3\pi^2 \rho_p(0))^{1/3}. \quad (7)$$

In any case, we only need to know the proton density  $\rho_p(r)$  to obtain  $k_F^p$ . We will use below Eq. (6) for the calculation of the Fermi momentum. We note that the following results are not sensitive to the exact value of  $k_F^p$ , and are almost unchanged if Eq. (7) is used instead of Eq. (6).

We now use these results to extract the value of the  $pp$  contact for any nucleus using only its charge distribution. Since  $\rho_{pp}$  should be well described by  $\rho_{pp}^F$  for  $r > r_0 \approx 0.9$  fm and by the contact expression for  $r < r_0$ , we can extract the value of  $C_{pp}^0$  by only requiring the continuity of  $\rho_{pp}$  at  $r = r_0$ . This gives the relation

$$C_{pp}^0 = \frac{\rho_{pp}^F(r_0)}{|\varphi_{pp}^0(r_0)|^2}, \quad (8)$$

which is our new relation that connects the charge distribution and the  $pp$  contact. We recall that for calculating  $\rho_{pp}^F$  we only need to know the point-proton density  $\rho_p(r)$  (or the charge distribution), and that  $\varphi_{pp}^0$  is simply calculated by solving the two-nucleon Schrodinger equation. The ratio of  $pp$  contacts of two nuclei,  $X_1$  and  $X_2$ , is then given by

$$\frac{C_{pp}^0(X_1)}{C_{pp}^0(X_2)} = \frac{\rho_{pp}^{F,X_1}(r_0)}{\rho_{pp}^{F,X_2}(r_0)}, \quad (9)$$

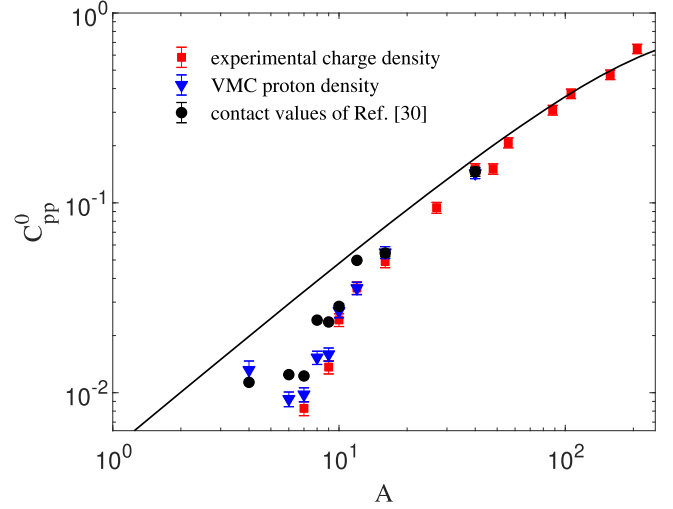


**Fig. 2.** The  $pp$  contact values as a function of  $A$ , extracted based on Eq. (8), using the VMC proton density and the experimental charge density (blue triangles and red squares, correspondingly). Previously extracted values of the  $pp$  contacts are shown as black points (taken from table 1 of Ref. [30], without the  $A/2$  normalization). The black line is a fit of the form  $C_{pp}^0 = bZ^2/A$ , with  $b = 0.02$ . See the text for more details.

where  $\rho_{pp}^{F,X}$  is the uncorrelated  $pp$  density of nucleus  $X$ , with Fermi corrections. The universal two-body functions cancel in taking the ratio so that this contact ratio is independent of the model of the nucleon-nucleon potential.

The calculations shown in Fig. 1 imply that this new relation can be used to extract the value of the  $^{40}\text{Ca}$   $pp$  contact  $C_{pp}^0$  using its charge distribution. Inspecting the figure we see that the VMC results are well reproduced by the contact expression for  $r \leq 1$  fm and by  $\rho_{pp}^F$  for  $r \geq 2$  fm. In between we see a discrepancy of about 10–20% which we attribute to the contribution of  $\ell \neq 0$  channels neglected here and to three-body correlations. The use of the infinite nuclear-matter approximation might also have some contribution to this difference. We thus expect our error to be of the order of 10%. To get a more concrete estimate for the uncertainties in  $C_{pp}^0$  we vary  $r_0$  between 0.8 fm to 1 fm.

We next use Eq. (8) to extract the  $pp$  contacts of different nuclei. For nuclei up to  $A = 40$ , we can use the VMC calculations for the point-proton density, or the experimental data [35]. For heavier nuclei, only experimental data is available. Using this new method, the extracted  $pp$  contacts for various nuclei, ranging from  $^4\text{He}$  to  $^{208}\text{Pb}$ , are presented in Fig. 2, as a function of the number of nucleons  $A$ , in log-log scale. One can see that the flexibility of using either the VMC point-proton densities or experimental charge densities has little impact on the extracted values of the contacts. Contact values of  $A \leq 40$  nuclei that were previously extracted by fitting directly the short-distance part of the VMC two-body densities in coordinate space [30] are also presented in the figure. Overall good agreement is observed between these values and the values extracted here using the charge density. This strengthens the validity of the relation between the nuclear contacts and the charge density. We note that some deviations are seen for the light nuclei ( $A \leq 9$ ). This is expected due to the use of the nuclear matter expression in deriving Eq. (4). Thus, our model for the  $pp$  pair-density is best suited for application to medium to heavy nuclei. Notice that both  $^{40}\text{Ca}$  and  $^{48}\text{Ca}$  are presented in the figure and have similar  $pp$  contact values, given the uncertainties. The black line in the figure represents a fit of the form  $C_{pp}^0(A) = bZ^2/A$ ,

where  $b$  is a fitting parameter, and the value of  $Z$  was estimated using the relation

$$Z \approx \frac{A}{2} \left[ 1 - \frac{a_c A^{2/3}}{4a_A} \right] \approx \frac{A}{2} \left[ 1 - 0.0075 A^{2/3} \right], \quad (10)$$

obtained from the semi-empirical mass formula looking for the value of  $Z$ , for a given  $A$ , that minimize the mass.  $a_c \approx 0.711$  MeV and  $a_A \approx 23.7$  MeV are the coefficients of the Coulomb and asymmetry terms in the mass formula. The fitted value of  $b$  is 0.02. The black line seems to describe the data well, especially for medium size and heavy nuclei. This indicates that the  $pp$  contacts, i.e. the probability of finding a correlated  $pp$  pair in the nucleus, scale like  $Z^2/A$ . Similar scaling,  $C_{pp}^0 \propto Z$ , was postulated in [28] and can also describe these results reasonably well. A qualitative explanation of the  $Z^2/A$  behavior is that the number of pairs must be multiplied by the probability for a proton to be at a given location, which is the inverse of the nuclear volume, i.e., the inverse of  $A$  assuming constant density. This behavior is significantly different from the naive combinatorial scaling of the number of  $pp$  pairs.

To better understand this scaling of the  $pp$  contact values, we examine a simple model, similar to the Fermi-gas model, in which the nucleus is a sphere with volume  $V$ . The proton density is just  $Z/V$  inside the nucleus radius, and vanishes outside. In this case, for  $V \rightarrow \infty$ , the integration over  $R$  in  $\rho_{pp}^{UC}$  just gives additional factor of  $V$ , and we get

$$\rho_{pp}^F(r) \approx \frac{1}{2} \frac{Z^2}{V} \left[ 1 - \frac{1}{2} \left( \frac{3j_1(k_F^p r)}{k_F^p r} \right)^2 \right] \quad (11)$$

We expect this result to hold for heavy nuclei. We can use  $k_F^p = (3\pi^2 \rho_p)^{1/3} = (3\pi^2 Z/V)^{1/3}$ . For the volume of the nucleus we can use the approximate relation  $V = \frac{4\pi}{3} R_0^3 A$ , where  $R_0 \approx 1.2$  fm. Using these relations, it turns out that the term in the large brackets in Eq. (11) for  $r = r_0$ , is almost constant for all nuclei, i.e. approximately  $A$ -independent, and equals approximately  $3/5$ . Eventually, following Eq. (8), we get

$$C_{pp}^0 \approx \frac{9}{40\pi} \frac{1}{R_0^3} \frac{1}{|\varphi_{pp}^0(r_0)|^2} \frac{Z^2}{A} \approx (0.023 \pm 0.002) \frac{Z^2}{A}, \quad (12)$$

using  $|\varphi_{pp}^0(r_0)|^2 \approx 1.8311 \text{ fm}^{-3}$  for the AV18 potential, and  $r_0 = 0.9$  fm, and estimating the error by varying  $r_0$  between 0.8 fm to 1 fm. Using this simple model, we have obtained here the  $Z^2/A$  scaling of the  $C_{pp}^0$  contacts, seen in Fig. 2. The numerical coefficient obtained here also agrees with the fitted value of  $b$ , presented above.

As mentioned before, in principle, the point-proton density should be used in Eq. (2) and not the charge density. A possible way for calculating the point-proton density from the experimental charge density is described in Ref. [42]. Calculating the point density of  $^{40}\text{Ca}$  based on Eqs. (17) and (18) of that paper, and assuming the neutron density is the same as the proton density, leads to a small correction of less than 10% in the extracted  $pp$  contact of  $^{40}\text{Ca}$ . The correction for heavier nuclei is expected to be even smaller.

We have shown here that the  $pp$  contacts can be evaluated using only the charge density. We will now present an even more surprising relation: the connection between the charge density and neutron–proton SRCs. To this end we focus on symmetric ( $N = Z$ ) nuclei. For  $pp$  pairs we had to consider only one channel, the spin-zero channel. In contrast, for  $pn$  pairs we have a more complicated situation as there are two leading SRC channels: the spin-zero

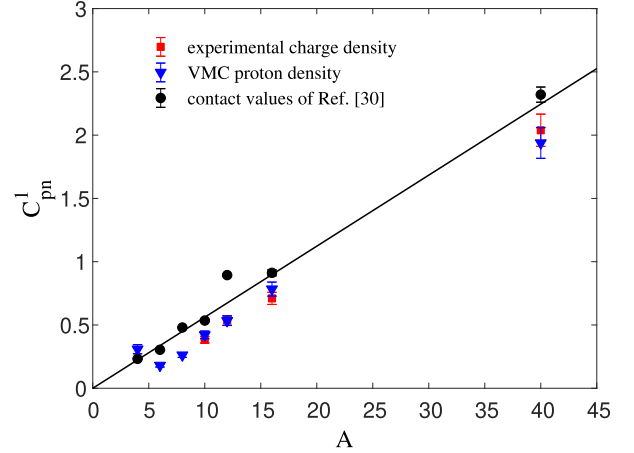


**Fig. 3.** The  $pn$  deuteron contact values as a function of  $A$ , for symmetric nuclei, extracted using Eq. (16), using the VMC point-proton densities and experimental charge densities (blue triangles and red squares, correspondingly). Previously extracted values for symmetric nuclei are shown as black points (taken from table I of Ref. [30], without the  $A/2$  normalization). The black line is a fit of the form  $C_{pn}^1(A) = aA$ , resulting  $a = 0.056$ .

channel and the spin-one channel (the deuteron channel). To resolve this problem we note that, due to isospin symmetry [30], for symmetric nuclei the  $pp$  and  $pn$  spin-zero contacts are the same.

As before, also for  $pn$  pairs we start with the uncorrelated two-body density given by

$$\rho_{pn}^{UC}(\mathbf{r}) = \int d^3R \rho_p(\mathbf{R} + \mathbf{r}/2) \rho_n(\mathbf{R} - \mathbf{r}/2). \quad (13)$$

The one-body neutron density  $\rho_n(\mathbf{r})$  is not as accessible experimentally as the proton density, however for symmetric nuclei, isospin symmetry implies that  $\rho_n(\mathbf{r}) \approx \rho_p(\mathbf{r})$ . It follows that for symmetric nuclei  $\rho_{pn}^{UC}(\mathbf{r}) \approx \rho_{pp}^{UC}(\mathbf{r})$ . Since protons and neutrons are distinguishable, there is no correction due to the Fermi statistics here. At small distances we use the contact relation for the  $pn$  density [30]

$$\rho_{pn}(r) = C_{pn}^0 |\varphi_{pn}^0(r)|^2 + C_{pn}^1 |\varphi_{pn}^1(r)|^2. \quad (14)$$

As for the  $pp$  case, we expect both the contact relation and the uncorrelated expression to describe reasonably well the full  $pn$  density around  $r = r_0$ . Thus, by requiring only the continuity of the  $pn$  density at  $r_0$ , we find that

$$C_{pn}^0 |\varphi_{pn}^0(r_0)|^2 + C_{pn}^1 |\varphi_{pn}^1(r_0)|^2 = \rho_{pn}^{UC}(r_0). \quad (15)$$

For symmetric nuclei,  $C_{pn}^0 \approx C_{pp}^0$ , and also, generally,  $\varphi_{pn}^0(r) \approx \varphi_{pp}^0(r)$ . Thus, utilizing Eq. (8) we obtain

$$C_{pn}^1 = \frac{\rho_{pn}^{UC}(r_0) - \rho_{pp}^F(r_0)}{|\varphi_{pn}^1(r_0)|^2}. \quad (16)$$

This relation indicates that the ratio of two  $pn$  deuteron-channel contacts, for two symmetric nuclei, does not depend on the potential, similar to Eq. (9). Eq. (16) can be used to extract the values of the  $pn$  deuteron-channel contacts for symmetric nuclei, using only the proton density as an input. The results are presented in Fig. 3 for several symmetric nuclei ( $A \leq 40$ ). The values were extracted using both the VMC point-proton densities and experimental charge densities. The values extracted using these two possibilities agree with each other for each nucleus. The extracted

values are also compared to previous values extracted by fitting to the VMC densities directly [30]. Fair agreement is observed. The extraction of the  $pn$  contact values using the charge density seems to slightly underestimate the values of the contact for  $A \leq 40$ . The uncertainties of the contacts extracted here are obtained by varying  $r_0$  between 0.8 fm and 1 fm. The black line is a fit of the form  $C_{pn}^1(A) = aA$ , yielding

$$C_{pn}^1(A) = (0.056 \pm 0.001)A. \quad (17)$$

We can analyze the  $pn$  deuteron-contact scaling as we did for the  $pp$  case. Using the same model, we get for symmetric nuclei  $C_{pn}^1(A) \approx (0.073 \pm 0.008)A$ , where we have used  $|\varphi_{pn}^1(r_0)|^2 = 0.3335 \text{ fm}^{-3}$  for  $r = 0.9 \text{ fm}$  and  $R_0 = 1.2 \text{ fm}$ . This is a linear relation between  $C_{pn}^1(A)$  and  $A$ , in agreement with Fig. 3. The coefficient obtained using this simple model is larger than the fitted value of  $a$  presented above. Notice that Fig. 3 includes only  $A \leq 40$  nuclei while we expect this model to work for heavy nuclei, as seen from the fit in Fig. 2. This can explain the difference obtained here between the two values of  $a$ .

The  $A$ -dependence of the deuteron-channel contact was studied before, using a relation between the contacts and the Levinger constant [27,28,33]. The Levinger constant  $L$  relates the photo-absorption cross section of a nucleus  $A$ ,  $\sigma_A(\omega)$ , with the same cross section for the deuteron,  $\sigma_d(\omega)$ , [43]

$$\sigma_A(\omega) = L \frac{NZ}{A} \sigma_d(\omega). \quad (18)$$

Here,  $100 \text{ MeV} < \hbar\omega < 200 \text{ MeV}$  is the photon energy. The idea that the photon is absorbed by a  $pn$  pair was used to show that the Levinger constant is related to the probability to find a correlated  $pn$  pair in a nucleus  $A$  relative to that of the deuteron [27,33]. Using the contacts, this relation can be written as

$$C_{pn}^1(A) = L \frac{NZ}{A} C_{pn}^1(d). \quad (19)$$

The deuteron's spin-one contact  $C_{pn}^1(d)$  describes the probability to find a correlated pair in the deuteron with momentum above  $k_F$ . For the AV18 potential, and  $k_F = 1.3 \text{ fm}^{-1}$ ,  $C_{pn}^1(d) = 0.0475 \pm 0.0005$ . Using the experimental estimation of  $L = 5.5 \pm 0.2$  [27] we obtain

$$C_{pn}^1(A) = (0.26 \pm 0.01) \frac{NZ}{A} = (0.065 \pm 0.003)A, \quad (20)$$

where the last equality holds for symmetric nuclei. Thus, comparing to Eq. (17), there is agreement to within 10% between the experimental value of the Levinger constant and the contact values extracted using the charge density.

In [30] the nuclear contacts were related to the high-momentum scaling factor  $a_2 = (2/A)\sigma_A/\sigma_D$ , that is extracted from inclusive electron scattering cross-section ratios, in a similar fashion to the Levinger constant. Fomin et al. [4], evaluated  $a_2$  from inclusive experiments carried out at Jefferson laboratory, and have found that for medium-size and heavy nuclei it is roughly a constant  $a_2 = 4.3 \pm 0.3$ , after correcting for center-of-mass motion. Utilizing this value we get  $C_{pn}^1(A) = (0.085 \pm 0.006)A$  for symmetric nuclei, a value somewhat larger than the other extractions. For example, using the value of  $C_{pp}^0$  of  $^{40}\text{Ca}$ , presented in Fig. 2, and the interpolated value of  $a_2 \approx 4.15$  we get  $C_{pn}^1(^{40}\text{Ca}) \approx 3.5$ , which is more than 30% larger than the value presented in Fig. 3. The use of the value of  $a_2$  without the center-of-mass correction of Ref. [4] leads to a larger discrepancy. These discrepancies require further investigation.

To emphasize the implications of these results, we focus on the example of  $^{40}\text{Ca}$ . Based on Figs. 2 and 3, we have  $C_{pn}^1(^{40}\text{Ca}) \approx 2.2$  and  $C_{pp}^0(^{40}\text{Ca}) \approx 0.15$ . Thus, the ratio of total correlated  $pn$  deuteron pairs to correlated  $pp$  pairs (with relative momentum above  $k_F$ ) in  $^{40}\text{Ca}$  is  $C_{pn}^1(^{40}\text{Ca})/C_{pp}^0(^{40}\text{Ca}) \approx 15$ . This agrees with the known dominance of correlated  $pn$  pairs over  $pp$  pairs [7,9]. As a result, we are led to the conclusion that the  $pn$  dominance of SRC pairs can be explained using only the charge distribution. If we use the scaling of the  $pp$  contacts obtained above, and the scaling of the  $pn$  contacts based on the relation to the Levinger constant, we obtain

$$\frac{C_{pn}^1}{C_{pp}^0} = \frac{LC_{pn}^1(d)N}{bZ} \approx 13 \frac{N}{Z}. \quad (21)$$

This provides a prediction for the scaling of the ratio between the amount of SRC  $pn$  (deuteron) pairs and  $pp$  pairs, valid for medium-heavy nuclei, that should be checked when sufficient experimental data will be available. We note that the numerical factor might be model dependent but the  $N/Z$  scaling should be model independent.

The same idea can be applied to not only the  $pn$  to  $pp$  ratio but also to other nuclear quantities, such as high momentum tails and the Coulomb sum rule, which can be described using the nuclear contacts. On the other hand, some properties of nuclear SRCs, such as the center-of-mass momentum distribution of the pairs [44], cannot be explored using this model.

To conclude, charge density and nuclear SRCs seem naively to be two unrelated aspects of nuclear systems. Nevertheless, the use of the generalized nuclear contact formalism leads to the derivation of a direct relation between the two. Namely, we have been able to extract the nuclear contacts, which are proportional to the probability of finding pairs of nucleons in a close proximity in the nucleus, using only the charge density. The  $pp$  contacts for various nuclei, and the  $pn$  contacts for symmetric nuclei, are evaluated and compared to previously known values of the contacts, and a good agreement was observed. Since charge densities are known for many nuclei, this provides a useful way for extracting SRC properties of heavy nuclei, for which ab-initio calculations are presently almost impossible. This new relation also shows that the ratio of  $pp$  contacts, for two nuclei, does not depend on the choice of a particular nucleon-nucleon interaction. This holds also for the  $pn$  contacts of symmetric nuclei. The scaling of the  $pp$  and  $pn$  contacts is also discussed and identified, leading to a prediction regarding the  $pn$  to  $pp$  ratio of SRC pairs. The extracted values of the  $pn$  contacts seem to agree with a previous relation, connecting the Levinger constant and the contacts, and with the known  $pn$  dominance. The relation between the contacts and  $a_2$  requires further investigation.

The nuclear contacts are directly related to several nuclear quantities and reactions, such as the high-momentum tail of momentum distributions, high momentum-transfer and energy-transfer electron-scattering experiments sensitive to nuclear SRCs, the Coulomb sum-rule, and the properties of nuclear matter. The use of the new relations presented in this work can provide predictions for such sophisticated experiments and calculations for different nuclei using only the widely known charge distribution of each nucleus.

## Acknowledgements

This work was supported by the PAZY Foundation, by the U. S. Department of Energy Office of Science, Office of Nuclear Physics under Award Number DE-FG02-97ER-41014, the Batsheva de Rothschild Fellowship of the Israel Academy of Sciences and Humani-

ties, and the Shaoul Fellowship of the Sackler Institute of Tel-Aviv University.

## References

- [1] L.L. Frankfurt, M.I. Strikman, D.B. Day, M. Sargsyan, *Phys. Rev. C* 48 (1993) 2451.
- [2] K. Egiyan, et al., *Phys. Rev. C* 68 (2003) 014313.
- [3] K. Egiyan, et al., *Phys. Rev. Lett.* 96 (2006) 082501.
- [4] N. Fomin, et al., *Phys. Rev. Lett.* 108 (2012) 092502.
- [5] A. Tang, et al., *Phys. Rev. Lett.* 90 (2003) 042301.
- [6] E. Piasetzky, M. Sargsian, L. Frankfurt, M. Strikman, J.W. Watson, *Phys. Rev. Lett.* 97 (2006) 162504.
- [7] R. Subedi, et al., *Science* 320 (2008) 1476.
- [8] I. Korover, et al., *Phys. Rev. Lett.* 113 (2014) 022501.
- [9] O. Hen, et al., CLAS Collaboration, *Science* 346 (2014) 614.
- [10] H. Baghdasaryan, et al., *Phys. Rev. Lett.* 105 (2010) 222501.
- [11] R. Shneor, et al., *Phys. Rev. Lett.* 99 (2007) 072501.
- [12] R. Schiavilla, R.B. Wiringa, Steven C. Pieper, J. Carlson, *Phys. Rev. Lett.* 98 (2007) 132501.
- [13] M. Alvioli, C. Ciofi degli Atti, H. Morita, *Phys. Rev. Lett.* 100 (2008) 162503.
- [14] H. Feldmeier, W. Horiuchi, T. Neff, Y. Suzuki, *Phys. Rev. C* 84 (2011) 054003.
- [15] M. Alvioli, C. Ciofi degli Atti, L.P. Kaptari, C.B. Mezzetti, H. Morita, *Phys. Rev. C* 87 (2013) 034603.
- [16] A. Rios, A. Polls, W.H. Dickhoff, *Phys. Rev. C* 89 (2014) 044303.
- [17] C. Ciofi degli Atti, S. Simula, L.L. Frankfurt, M.I. Strikman, *Phys. Rev. C* 44 (1991) R7(R).
- [18] C. Ciofi degli Atti, S. Simula, *Phys. Rev. C* 53 (1996) 1689.
- [19] C. Ciofi degli Atti, C.B. Mezzetti, H. Morita, *Phys. Rev. C* 95 (2017) 044327.
- [20] C. Ciofi degli Atti, H. Morita, *Phys. Rev. C* 96 (2017) 064317.
- [21] O. Hen, G.A. Miller, E. Piasetzky, L.B. Weinstein, *Rev. Mod. Phys.* 89 (2017) 045002.
- [22] C. Ciofi degli Atti, *Phys. Rep.* 590 (2015) 1.
- [23] N. Fomin, D. Higinbotham, M. Sargsian, P. Solvignon, *Annu. Rev. Nucl. Part. Sci.* 67 (2017) 129.
- [24] S. Tan, *Ann. Phys. (N. Y.)* 323 (2008) 2952; S. Tan, *Ann. Phys. (N. Y.)* 323 (2008) 2971; S. Tan, *Ann. Phys. (N. Y.)* 323 (2008) 2987.
- [25] E. Braaten, in: W. Zwerger (Ed.), *BCS-BEC Crossover and the Unitary Fermi Gas*, Springer, 2012.
- [26] G.A. Miller, *Phys. Lett. B* 777 (2018) 442.
- [27] R. Weiss, B. Bazak, N. Barnea, *Phys. Rev. Lett.* 114 (2015) 012501.
- [28] R. Weiss, B. Bazak, N. Barnea, *Phys. Rev. C* 92 (2015) 054311.
- [29] R. Weiss, N. Barnea, *Phys. Rev. C* 96 (2017) 041303(R).
- [30] R. Weiss, R. Cruz-Torres, N. Barnea, E. Piasetzky, O. Hen, *Phys. Lett. B* 780 (2018) 211.
- [31] M. Alvioli, C. Ciofi degli Atti, H. Morita, *Phys. Rev. C* 94 (2016) 044309.
- [32] R. Weiss, E. Pazy, N. Barnea, *Few-Body Syst.* 58 (2017) 9.
- [33] R. Weiss, B. Bazak, N. Barnea, *Eur. Phys. J. A* 52 (2016) 92.
- [34] R. Weiss, I. Korover, E. Piasetzky, O. Hen, N. Barnea, arXiv:1806.10217 [nucl-th], 2018.
- [35] H. De Vries, C.W. De Jager, C. De Vries, *At. Data Ann. Nucl. Data Tables* 36 (1987) 495.
- [36] R.B. Wiringa, V.G.J. Stoks, R. Schiavilla, *Phys. Rev. C* 51 (1995) 38.
- [37] R.B. Wiringa, R. Schiavilla, S.C. Pieper, J. Carlson, *Phys. Rev. C* 89 (2014) 024305.
- [38] D. Lonardoni, A. Lovato, S.C. Pieper, R.B. Wiringa, *Phys. Rev. C* 96 (2017) 024326.
- [39] R. Cruz-Torres, et al., *Phys. Lett. B* 785 (2018) 304.
- [40] J.W. Negele, *Phys. Rev. C* 1 (1970) 1260.
- [41] S.C. Pieper, V.R. Pandharipande, R.B. Wiringa, J. Carlson, *Phys. Rev. C* 64 (2001) 014001.
- [42] N. Rocco, C. Barbieri, *Phys. Rev. C* 98 (2018) 025501.
- [43] J.S. Levinger, *Phys. Rev.* 84 (1951) 43.
- [44] E.O. Cohen, et al., CLAS Collaboration, *Phys. Rev. Lett.* 121 (2018) 092501.